Topological Phases of Parafermions: A Model with Exactly Solvable Ground States

Fernando Iemini,[1,2] Christophe Mora,[3] and Leonardo Mazza[4]
[1]ICTP, Strada Costiera 11, I-34151 Trieste, Italy
[2]NEST, Scuola Normale Superiore and Istituto Nanoscienze-CNR, I-56126 Pisa, Italy
[3]Laboratoire Pierre Aigrain, École Normale Supérieure/PSL Research University, CNRS, Université Pierre et Marie Curie-Sorbonne Universités, Université Paris Diderot-Sorbonne Paris Cité, 24 rue Lhomond, 75231 Paris Cedex 05, France
[4]Département de Physique, École Normale Supérieure/PSL Research University, CNRS, 24 rue Lhomond, F-75005 Paris, France
(Received 2 November 2016; revised manuscript received 12 January 2017; published 25 April 2017)

Parafermions are emergent excitations that generalize Majorana fermions and can also realize topological order. In this Letter, we present a nontrivial and quasi-exactly-solvable model for a chain of parafermions in a topological phase. We compute and characterize the ground-state wave functions, which are matrix-product states and have a particularly elegant interpretation in terms of Fock parafermions, reflecting the factorized nature of the ground states. Using these wave functions, we demonstrate analytically several signatures of topological order. Our study provides a starting point for the nonapproximate study of topological one-dimensional parafermionic chains with spatial inversion and time-reversal symmetry in the absence of strong edge modes.

DOI: 10.1103/PhysRevLett.118.170402

Introduction.—The study of topological order (TO) is currently one of the most active research fields in condensed-matter physics. From the Affleck-Kennedy-Lieb-Tasaki (AKLT) model [1] to the Laughlin wave function [2], from the Kitaev chain [3] to the toric code [4], this study has always benefited from the development of exactly solvable models and of paradigmatic wave functions, whose detailed analysis permits the formation of a clear physical intuition, to be used in the understanding of complex experimental setups.

In this Letter, we focus on *parafermions*, a generalization of Majorana fermions [5]. After the experimental clarification that two zero-energy Majorana modes can be localized at the edges of a one-dimensional fermionic wire [6,7], the possibility of localizing parafermionic modes, and letting them interact, is currently under deep investigation. These excitations cannot appear in strictly one-dimensional spinless fermionic systems [8,9] but may emerge at the edge of a two-dimensional fractional topological insulator coupled to alternating ferromagnetic and superconducting materials [5,10–15], as well as in other nanostructures or models [16–24].

In these setups, one-dimensional chains of interacting parafermions arise, which, in certain circumstances, display TO and edge $\mathbb{Z}_N$ parafermionic modes [5,25–34]. Such edge modes are called strong when they commute with the Hamiltonian [35] and thereby generate an N-fold degeneracy in the entire spectrum and weak when the commutation property and associated degeneracy are restricted to the ground-state manifold. TO survives weak perturbations and hosts indistinguishably weak or strong modes [36]. The importance of parafermionic zero modes for topological quantum computation [37] motivates further investigations of these fractionalized systems.

In this Letter, we provide a nontrivial family of parafermionic models for which the properties of the ground states can be exactly characterized. These models are gapped, display TO, have spatial inversion and time-reversal symmetries, and feature weak edge modes; they thus belong to the same symmetry class for which weak edge modes have been discussed so far with numerical and perturbative analytical methods [28,31,36], with the advantage of being easy to handle. We analytically establish several key signatures of TO which can be easily extracted from the wave functions: (i) the presence of nonlocal edge-edge correlations, (ii) the indistinguishability of ground states by a symmetry-preserving local observable, (iii) the fact that only operators living at the edges are able to permute ground states, and (iv) the N-fold degeneracy of the entanglement spectrum [26]. We also motivate the existence of weak edge modes.

The analysis rests on an intuitive "particlelike" picture of parafermions [38,39], that naturally leads to a formulation of the ground states in terms of matrix-product states (MPSs) [40]. Our model is thus a simple platform for the direct study of TO in parafermionic systems, which is particularly valuable given even the absence of a noninteracting and exactly solvable limit (see, however, Ref. [34]). For simplicity, we present our discussion in the case of $\mathbb{Z}_3$ parafermions, but the construction can be easily generalized to $\mathbb{Z}_N$ parafermions. A similar study has been discussed in the fermionic ($\mathbb{Z}_2$) case [41].

The model.—We consider a one-dimensional chain with length L of $\mathbb{Z}_3$ parafermions. Each lattice site k is associated with two parafermionic operators $\hat{\gamma}_{2k-1}$ and $\hat{\gamma}_{2k}$, which satisfy the following properties: $\hat{\gamma}_j^3 = 1$ and $\hat{\gamma}_j^\dagger = \hat{\gamma}_j^2$; moreover, $\hat{\gamma}_j \hat{\gamma}_l = \omega \hat{\gamma}_l \hat{\gamma}_j$ for $j < l$, where

$\omega = e^{2\pi i/3}$. We consider the following model, $\hat{H} = \hat{H}_0 + b\hat{H}_1 + b^2\hat{H}_2$:

$$\hat{H}_0 = \sum_j (-f\omega^* \hat{\gamma}^\dagger_{2j-1}\hat{\gamma}_{2j} - J\omega\hat{\gamma}_{2j}\hat{\gamma}^\dagger_{2j+1} + \text{H.c.}); \tag{1a}$$

$$\hat{H}_1 = -J\sum_j (\hat{A}_j \hat{\gamma}^\dagger_{2j+1} + \hat{\gamma}_{2j}\hat{B}^\dagger_{j+1} + \text{H.c.}); \tag{1b}$$

$$\hat{H}_2 = -J\sum_j (\omega^* \hat{A}_j \hat{B}^\dagger_{j+1} + \text{H.c.}); \tag{1c}$$

where $\hat{A}_j = (\hat{\gamma}_{2j-1} + \hat{\gamma}^\dagger_{2j-1}\hat{\gamma}^\dagger_{2j})$ and $\hat{B}_j = (\hat{\gamma}_{2j} + \hat{\gamma}^\dagger_{2j}\hat{\gamma}^\dagger_{2j-1})$.

For $b = 0$, $\hat{H}$ reduces to the well-known parafermionic version of the three-state Potts quantum chain [42–47]. For positive f and J, such a model has a topological phase transition at $f = J$ between a topological phase with zero boundary modes ($f < J$) and a trivial phase ($f > J$). For $f = 0$, the Hamiltonian is the sum of commuting and frustration-free terms and displays TO.

Quasi-exactly-solvable line.—The Hamiltonian (1) has a quasi-exactly-solvable line (where only the ground state but not the excited states can be exactly computed) parametrized by $\phi \in \mathbb{R}$:

$$\frac{f}{J} = -6\frac{1 - e^{-2\phi}}{(1 + 2e^{-\phi})^2}; \qquad b = \frac{1 - e^{-\phi}}{1 + 2e^{-\phi}}, \tag{2}$$

which is plotted in Fig. 1. We consider open boundary conditions; the properties of the ground states are exactly computable once the boundary term is introduced:

$$\hat{H}_B = +\frac{f}{2}(\omega^* \hat{\gamma}^\dagger_1 \hat{\gamma}_2 + \omega^* \hat{\gamma}^\dagger_{2L-1}\hat{\gamma}_{2L} + \text{H.c.}). \tag{3}$$

This term does not change the thermodynamics of the model and produces modifications which scale as L^{-1}, which are negligible in the thermodynamic limit.

We begin by considering the point $\phi = 0$. Here, the Hamiltonian can be rewritten in the following expressive form: $\hat{H} + \hat{H}_B = -2J(L-1)\hat{\mathbb{1}} + J\sum_{j=1}^{L-1} \hat{\ell}^\dagger_j \hat{\ell}_j$, where $\hat{\ell}_j = \hat{\gamma}^\dagger_{2j} - \omega\hat{\gamma}^\dagger_{2j+1}$. The first term, inessential, is proportional to the identity. The second part, instead, is non-negative, and its three ground states $|g_{i,\phi=0}\rangle$ $(i = 0,\ 1,\ 2)$ are characterized by $\hat{\ell}_j |g_{i,\phi=0}\rangle = 0$.

In order to visualize this result in solely parafermionic terms, we employ the "Fock parafermions" $\{\hat{C}_j\}_{j=1}^L$: $\hat{\gamma}_{2j-1} = \omega(\hat{C}_j + \hat{C}^{\dagger 2}_j)$ and $\hat{\gamma}_{2j} = \hat{C}_j \omega^{\hat{N}_j} + \hat{C}^{\dagger 2}_j$, where $\hat{N}_j = \hat{C}^\dagger_j \hat{C}_j + \hat{C}^{\dagger 2}_j \hat{C}^2_j$ is the number operator [38]. The Fock-parafermion operators are a generalization of canonical Fermi operators and satisfy, among others, the following commutation relations: $\hat{C}^3_j = 0$ and $\hat{C}_j\hat{C}_k = \omega\hat{C}_k\hat{C}_j$ $(j < k)$. They are associated with a local Fock space where a number of Fock parafermions between 0 and 2 can be accommodated and are amenable to a simple picture of particlelike excitations. The Hilbert space of the whole chain is spanned by all Fock states $|\{n_j\}\rangle$, where $n_j \in \{0, 1, 2\}$ is the number of parafermions at site j.

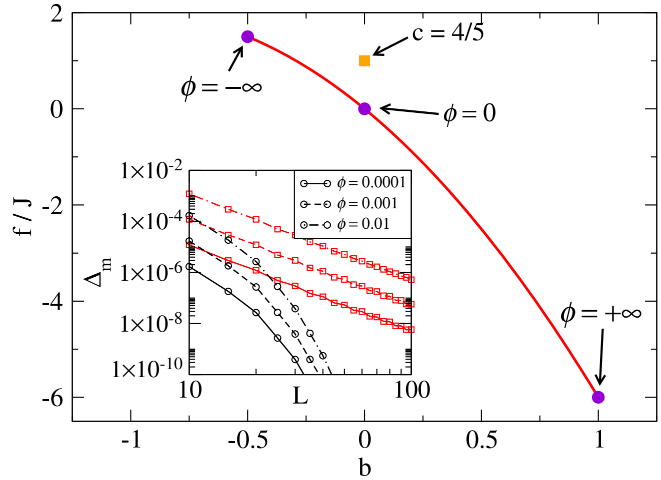

FIG. 1. Phase space of the model (1). The ground state is exactly solvable along the red line, which is parametrized ϕ according to Eq. (2). The points $\phi = \pm\infty$ and $\phi = 0$ are highlighted. For better reference, the well-studied critical point $f = J$, $b = 0$ with central charge $c = 4/5$ is also highlighted. Inset: Perturbative analysis of the size scaling of the degeneracies Δ_m of the first three excited states ($m = 1$, black circles) and of a higher excited triplet ($m = 4$, red squares), exhibiting, respectively, exponential and polynomial energy splitting. The polynomial scaling demonstrates the absence of strong edge modes. Three values of ϕ are considered: $\phi = 10^{-4}$ (solid line), $\phi = 10^{-3}$ (dashed line), and $\phi = 10^{-2}$ (dashed-dotted line).

The three ground states read

$$|g_{i,\phi=0}\rangle = \frac{1}{\sqrt{3^{L-1}}} \sum_{\substack{\{n_j\}\text{such that} \\ \sum_j n_j \equiv i(\text{mod}3)}} |\{n_j\}\rangle, \qquad i = 0, 1, 2. \tag{4}$$

They are the equal-amplitude superposition of all Fock states with a number N of Fock parafermions such that $N \equiv i(\text{mod}3)$. These states are similar to the Rokhsar-Kivelson states proposed in resonant valence-bond liquids [48]. Such states are, in fact, ubiquitous in the study of topological phases of matter, and they can also be encountered in the two- and three-dimensional toric code [4,49], in the AKLT model [1], or in the study of topological Majorana zero-energy modes [3,41,50,51]. The proof of Eq. (4) is obtained by expanding $\hat{\ell}_j = \omega^{-\hat{N}_j}\hat{C}^\dagger_j - \hat{C}^\dagger_{j+1} + \hat{C}^2_j - \hat{C}^2_{j+1}$ and explicitly inspecting that $\hat{\ell}_j|g_{i,\phi=0}\rangle = 0$. Excited states are obtained by applying the operators $\hat{\ell}^\dagger_j$ to the states $|g_{i,\phi=0}\rangle$ and normalizing, which demonstrates the presence of a gap $3J$ [52].

We now move to $\phi \neq 0$. We claim that the ground states are given by

$$|g_{i,\phi}\rangle = \frac{\hat{Z}_{-\phi}|g_{i,\phi=0}\rangle}{\sqrt{\langle g_{i,\phi=0}|\hat{Z}_{-2\phi}|g_{i,\phi=0}\rangle}}, \qquad (5)$$

where $\hat{Z}_\phi = e^{\phi\hat{N}/3}$ is a Hermitian, invertible, but nonunitary operator, $\hat{N} = \sum_j \hat{N}_j$ being the total number of parafermions in the chain. We prove our claim by constructing a parent Hamiltonian for the states $|g_{i,\phi}\rangle$ and then showing that it coincides with $\hat{H} + \hat{H}_B$, as given by Eqs. (1) and (3), apart from constant terms. We introduce a set of local operators $\hat{L}_{j,\phi} = \hat{Z}_{-\phi}\hat{\ell}_j\hat{Z}_\phi$; one easily verifies that acting with the parent Hamiltonian

$$\hat{H}_\phi = J\sum_{j=1}^{L-1} \hat{L}^\dagger_{j,\phi}\hat{L}_{j,\phi} \qquad (6)$$

on the states $|g_{i,\phi}\rangle$ gives zero. The model is not fully solvable and the different terms in Eq. (6) do not commute, except for $\phi = 0$. Nevertheless, $\hat{H}_\phi$ is a strictly nonnegative operator which completes the proof that $|g_{i,\phi}\rangle$ are ground states. More explicitly, the operators $\hat{L}_{j,\phi}$ take the form $\hat{L}_{j,\phi} = (e^{2\phi/3}/3)[\hat{\mathcal{W}}_{j,\phi}\hat{\gamma}^\dagger_{2j} - \omega\hat{\mathcal{W}}_{j+1,\phi}\hat{\gamma}^\dagger_{2j+1}]$, with

$$\hat{\mathcal{W}}_{j,\phi} = (1 + 2e^{-\phi}) + (1 - e^{-\phi})(\omega\hat{\gamma}^\dagger_{2j-1}\hat{\gamma}_{2j} + \text{H.c.}),$$

such that $\hat{H}_\phi$ coincides with the starting Hamiltonian (1) and the parametrization (2). The Hamiltonian remains time-reversal invariant (a detailed discussion is in Ref. [52]), as can be inferred by the fact that $\hat{N}_j$ satisfies such symmetry. Indeed, in the usual parafermionic language $\hat{N}_j = 1 + [(\omega^* - \omega)\hat{\gamma}^\dagger_{2j-1}\hat{\gamma}_{2j} + \text{H.c.}]/3$, and, since $\mathcal{T}$ is antiunitary and maps $\mathcal{T}[\hat{\gamma}^\dagger_{2j-1}\hat{\gamma}_{2j}] = \hat{\gamma}^\dagger_{2j}\hat{\gamma}_{2j-1}$, the invariance follows.

Ground-state properties.—We now turn to the analytical characterization of the $|g_{i,\phi}\rangle$. In the Fock-parafermion representation, the ground states take a particularly simple form:

$$|g_{i,\phi}\rangle = \frac{1}{\sqrt{\mathcal{N}_{L,\phi,i}}} \sum_{\substack{\{n_j\}\text{such that}\\ \sum_j n_j \equiv i (\text{mod} 3)}} e^{-\phi(\sum_j n_j)/3}|\{n_j\}\rangle, \qquad (7)$$

where the normalization constants $\mathcal{N}_{L,\phi,i}$ have an analytical expression. Comparing with the states in Eq. (4), the coefficients of the different Fock states now depend exponentially on the number of parafermions: The perturbation is effectively acting as a chemical potential which modifies the average number of particles.

Below, we take advantage of the relative simplicity of the ground-state expressions (7) to compute analytically and exactly various correlation functions. We begin by determining the correlation length of the states $|g_{i,\phi}\rangle$ through a $\mathbb{Z}_3$-preserving correlation function, for instance, $G_i(j,l) = \langle g_{i,\phi}|\hat{C}^{\dagger 2}_j\hat{C}^2_l|g_{i,\phi}\rangle$. The peculiar nature of the ground states makes it translationally invariant even for open boundary conditions: $G_i(j,l) = G_i(j-l)$. As displayed in Fig. 2, it exhibits an exponential decay $\sim\exp(-|j-l|/\xi)$ for $|j-l| < L/2$. ξ is the correlation length:

$$\xi^{-1} = \ln\left|\frac{1 + e^{-2\phi/3} + e^{-4\phi/3}}{1 + \omega e^{-2\phi/3} + \omega^* e^{-4\phi/3}}\right|; \qquad (8)$$

it is plotted in Fig. 2 as a function of ϕ. It is zero at $\phi = 0$, corresponding to a renormalization group fixed point, and diverges in the limits $\phi \to \pm\infty$. Thus, no phase transition occurs along the solvable line, apart from the extremal values.

It is instructive to show that the correlation length can also be computed in ways that are directly related to the topological nature of the ground states. We consider the expectation value of a $\mathbb{Z}_3$-preserving local operator, such as $\langle n\rangle_i = \langle g_{i,\phi}|\hat{N}_j|g_{i,\phi}\rangle$ (for the states $|g_{i,\phi}\rangle$, there is no dependence on j). In the thermodynamic limit, we analytically find

$$\langle n\rangle_i \to n(\phi) = \frac{e^{-2\phi/3} + 2e^{-4\phi/3}}{1 + e^{-2\phi/3} + e^{-4\phi/3}}, \qquad (9)$$

independent of i and j. At finite size L, we further obtain exponentially close values $\langle g_{i,\phi}|\hat{N}_j|g_{i,\phi}\rangle = n(\phi) + c_i e^{-L/\xi}$, as expected for TO [53], with the correlation length ξ of Eq. (8).

Getting back to the correlation function $G_i(j-l)$ in Fig. 2, we observe that the model displays nonlocal edge-edge correlations which survive in the thermodynamic limit. The importance of the edges is also revealed by

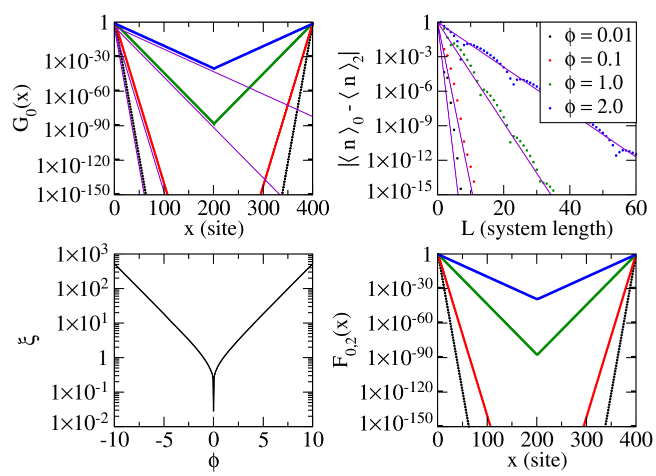

FIG. 2. (Top left) Correlation function $G_0(x)$ and (top right) $|\langle n\rangle_0 - \langle n\rangle_2|$ for several values of ϕ. Violet lines represent the exponential scalings extracted from the analytical formulas. (Bottom left) Correlation length ξ. (Bottom right) We show one typical example of the $\mathbb{Z}_3$-breaking observable $F_i(x)$ for $i = 0$.

$\mathbb{Z}_3$-breaking observables: In Fig. 2, we analytically compute and plot $F_i(j) = |\langle g_{i,\phi}|\hat{C}_j^\dagger|g_{i-1(\mathrm{mod}3),\phi}\rangle|$ for $i=0$, measuring how $\hat{C}_j^\dagger$ maps ground states with subsequent $\mathbb{Z}_3$ parities. The calculation reveals that it is nonzero only for j close to the boundaries with exponential decays again characterized by ξ. With this, we have so far encountered the first three signatures of TO and fractionalized boundary modes mentioned in the introduction, points (i)–(iii).

In order to confirm these findings, we consider the entanglement spectrum of the $|g_{i,\phi}\rangle$ states and prove its threefold degeneracy; see point (iv). In a bipartition of the system into a left part of length ℓ and a right part of length $L-\ell$, the ground state assumes the form

$$|g_{i,\phi}\rangle = \sum_{p=0}^{2}\sqrt{\frac{\mathcal{N}_{\ell,\phi,p}\mathcal{N}_{L-\ell,\phi,(i-p)\mathrm{mod}3}}{\mathcal{N}_{L,\phi,i}}}|g_{\phi,p}^{(\ell)}\rangle|g_{\phi,(i-p)\mathrm{mod}3}^{(L-\ell)}\rangle. \tag{10}$$

The reduced density matrix $\hat{\rho}_\ell$ is obtained by tracing out all sites of the right part. For $\ell \gg \xi$, the normalization constant $\mathcal{N}_{\ell,\phi,i}$ scales like $\sim(1/3)(1+e^{-2\phi/3}+e^{-4\phi/3})^\ell + \mathcal{O}(e^{-\ell/\xi})$, and the dependence on i appears only in the correction. Thus, for $\ell \gg \xi$ and $L-\ell \gg \xi$, the entanglement spectrum of the system is threefold degenerate, because for every $p = 0$, 1, 2 in Eq. (10) the coefficient of the sum reduces to $\sqrt{1/3}$, and the three states $|g_{\phi,p}^{(\ell)}\rangle$ equally participate to the reduced density matrix $\hat{\rho}_\ell$. In Fig. 3, we plot the typical behavior of the entanglement spectrum as a function of ℓ, the position of the bipartition: Close to the boundary ($\ell \ll \xi$), it consists of three different values, and away from it, they all collapse to 1/3. This expression also clarifies the gapped nature of the system through the area-law scaling of its von Neumann entropy $S(\hat{\rho}_\ell) = -\mathrm{tr}[\hat{\rho}_\ell \ln \hat{\rho}_\ell]$, plotted in Fig. 3. Explicit numerical calculations of the gap, obtained with the density-matrix renormalization group (DMRG) [54], reported in Fig. 3, confirm this fact.

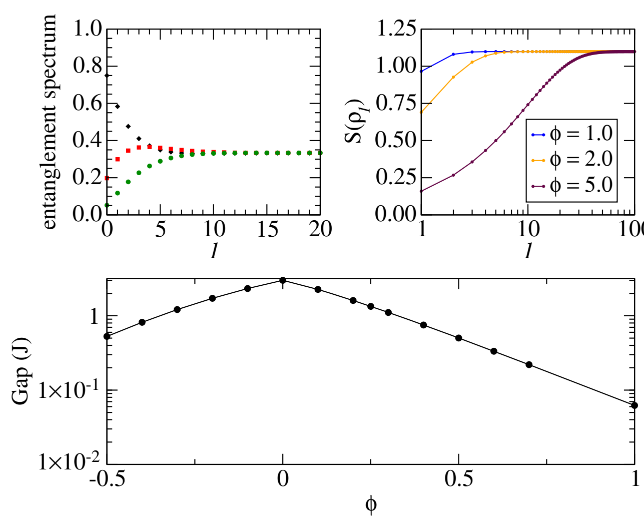

FIG. 3. Top left: Entanglement spectrum as a function of ℓ for $\phi = 2$. Top right: von Neumann entropy $S(\hat{\rho}_\ell)$ as a function of ℓ for three values of ϕ. At large ℓ, it saturates to a finite value corresponding to an area law. Bottom: DMRG calculation of the gap of the model obtained with length $L = 168$; the maximal number of retained states is $m = 250$.

Nature of the ground states.—This extended analytical analysis originates from the fact that the ground states are MPSs. They can be expressed as $|g_{i,\phi}\rangle = \sum_{n_1,\ldots,n_L} v_L^T A^{[n_1]}\ldots A^{[n_L]} v_{R,i}|n_1,\ldots n_L\rangle$ with the three matrices $A^{[j=0,1,2]} = (e^{-\phi/3}\hat{\sigma})^j$, where

$$\hat{\sigma} = \begin{pmatrix} 1 & 0 & 0 \\ 0 & \omega & 0 \\ 0 & 0 & \omega^2 \end{pmatrix}. \tag{11}$$

The parity i of the ground state is encoded in the left and right vectors, with $v_L^T = (1, \omega^i, \omega^{2i})$ and $v_R^T = (1,1,1)$ [40].

A particularly clear interpretation of the data which we have so far displayed comes from the observation that the ground states $|g_{i,\phi}\rangle$ are linear superpositions of three product states, as we are going to show. For $\phi = 0$, it can be explicitly verified that

$$|g_{i,\phi=0}\rangle = \frac{1}{\sqrt{3}}(\bigotimes_j|\tilde{0}_j\rangle + \omega^i\bigotimes_j|\tilde{1}_j\rangle + \omega^{2i}\bigotimes_j|\tilde{2}_j\rangle),$$

where $|\tilde{i}_j\rangle = (|n_j=0\rangle + \omega^{\tilde{i}}|n_j=1\rangle + \omega^{2\tilde{i}}|n_j=2\rangle)/\sqrt{3}$. The operator $\hat{Z}_\phi$ acts as a product operator over the different sites, without creating entanglement or correlations. We thus observe that, by applying $\hat{Z}_{-\phi}$ to the states $|g_{i,\phi=0}\rangle$ according to the prescription in Eq. (5), the states $\hat{Z}_{-\phi}\bigotimes_j|\tilde{i}_j\rangle$ retain a product nature. These states have zero correlation length and thus are fixed points of the renormalization group. This result can be considered an extension to three-state clock models of known results for spin-1/2 systems about the existence of factorized ground states [55,56], and it is intriguing to speculate that the peculiar properties of these models might extend to parafermionic chains [57].

Edge modes.—The parafermionic chain at $\phi = 0$ is characterized by (strong) edge modes, simply given by the operators $\hat{\chi}_1 = \hat{\gamma}_1$ and $\hat{\chi}_2 = \hat{\gamma}_{2L}$, permuting cyclically the ground states. As ϕ departs from zero, the edge modes $\hat{\chi}_{1,2}$ are continuously deformed but remain local. The calculation of $F_i(j)$ (see Fig. 2) already demonstrates that they keep a significant overlap with operators located close to the two ends of the chain. More generally, $\hat{\chi}_{1,2} = \hat{\mathcal{V}}_\phi\hat{\gamma}_{1,2L}\hat{\mathcal{V}}_\phi^\dagger$ are obtained from exact quasiadiabatic continuation [36] of $\hat{\gamma}_{1,2L}$ with the unitary transformation $\hat{\mathcal{V}}_\phi$ mapping the ground-state manifolds at zero and nonzero ϕ. Being unitary, $\hat{\mathcal{V}}_\phi$ preserves the parafermionic noncommutative algebra of $\hat{\chi}_{1,2}$ in the ground state, with $\langle g_{i,\phi}|\hat{\chi}_1|g_{i+1,\phi}\rangle = 1$ and $\langle g_{i,\phi}|\hat{\chi}_2|g_{i+1,\phi}\rangle = \omega^{2+i}$. It also preserves locality under the condition of quasiadiabaticity [36]. This program can be applied explicitly in perturbation with $\phi \ll 1$ and yields the left edge mode

$$\hat{\chi}_1 = \hat{\gamma}_1 + \alpha(\omega\gamma_3 - \gamma_2^\dagger\gamma_3^\dagger) + \alpha^*(\omega\gamma_1^\dagger\gamma_3\gamma_2 - \gamma_1^\dagger\gamma_3^\dagger) \quad (12)$$

to leading order in $\alpha = f/J - \omega b$. Parafermionic operators $\hat{\gamma}_j$ are also expected to enter the expression of $\hat{\chi}_1$ to the order of $j/2$ in f/J, b, so they are exponentially suppressed with the site index j. Similar considerations apply to the right mode $\hat{\chi}_2$. Finally, the form of $F_i(j)$ strongly suggests that the edge states $\hat{\chi}_{1/2}$ decay with the correlation length ξ at both ends of the chain.

The operators $\hat{\gamma}_1$ and $\hat{\gamma}_{2L}$ are strong edge modes for $\phi = 0$ as they commute with the Hamiltonian. It can be checked from the perturbative expression (12) that the commutation is lost at nonzero ϕ, yielding weak edge modes. Following Ref. [28], the low-energy part of the spectrum can be addressed at small ϕ by projecting the full Hamiltonian (1) onto single domain wall excitations, thus reducing the numerical complexity. In Fig. 1, we show the results of this analysis, where we plot $\Delta_m = \sqrt{\sum_{q\neq q'}(e_{m,q} - e_{m,q'})^2}$, and $e_{m,q}$ is the mth excited state which has a $\mathbb{Z}_3$ parity with value q. We find that the lowest triplets in the excitation spectrum ($m = 1$) exhibit an exponential closing with the system size, in contrast with higher triplet excitations ($m = 4$) where the closing is polynomial. This last observation rules out the presence of strong edge modes.

Conclusions.—In this Letter, we have presented a model for a one-dimensional parafermionic chain which displays TO and has quasi-exactly-solvable ground states. It beautifully exemplifies the physics proposed in Ref. [36] and allows for the explicit characterization of TO in the absence of strong boundary modes, providing an interesting starting point for developing a physical intuition of parafermionic systems, which is becoming particularly compelling in view of a forthcoming experimental realization. This is achieved with a systematic interpretation of our results in terms of Fock parafermions, a possibility which has not been fully explored yet. Understanding whether there are other parent Hamiltonians for the states $|g_{i,\phi}\rangle$ which are more physically relevant is an interesting perspective [58]; we also leave for the future further investigations concerning higher-dimensional lattices [25] as well as the complete mapping of the phase diagram of Hamiltonian (1).

We thank R. Fazio for encouraging us to perform this study. We also thank C. E. Bardyn, M. Burrello, M. Dalmonte, A. De Luca, M. Fagotti, G. Ortiz, N. Regnault, D. Rossini, and R. Santachiara for interesting discussions and comments. The numerical part of this work has been performed using the DMRG code released within the "Powder with Power" project. F. I. acknowledges financial support by the Brazilian agencies FAPEMIG, CNPq, and INCT-IQ. C. M. acknowledges support from Idex PSL Research University (ANR-10-IDEX-0001-02 PSL). L. M. was supported by LabEX ENS-ICFP: ANR-10-LABX-0010/ANR-10- IDEX-0001-02 PSL*.

[1] I. Affleck, T. Kennedy, E. H. Lieb, and H. Tasaki, Phys. Rev. Lett. **59**, 799 (1987).
[2] R. B. Laughlin, Phys. Rev. Lett. **50**, 1395 (1983).
[3] A. Y. Kitaev, Phys. Usp. **44**, 131 (2001).
[4] A. Y. Kitaev, Ann. Phys. (Amsterdam) **303**, 2 (2003).
[5] J. Alicea and P. Fendley, Annu. Rev. Condens. Matter Phys. **7**, 119 (2016).
[6] V. Mourik, K. Zuo, S. M. Frolov, S. R. Plissard, E. P. A. M. Bakkers, and L. P. Kouwenhoven, Science **336**, 1003 (2012).
[7] S. M. Albrecht, A. P. Higginbotham, M. Madsen, F. Kuemmeth, T. S. Jespersen, J. Nygård, P. Krogstrup, and C. M. Marcus, Nature (London) **531**, 206 (2016).
[8] A. M. Turner, F. Pollmann, and E. Berg, Phys. Rev. B **83**, 075102 (2011).
[9] L. Fidkowski and A. Y. Kitaev, Phys. Rev. B **83**, 075103 (2011).
[10] M. Barkeshli and X.-L. Qi, Phys. Rev. X **2**, 031013 (2012).
[11] N. H. Lindner, E. Berg, G. Refael, and A. Stern, Phys. Rev. X **2**, 041002 (2012).
[12] M. Cheng, Phys. Rev. B **86**, 195126 (2012).
[13] D. J. Clarke, J. Alicea, and K. Shtengel, Nat. Commun. **4**, 1348 (2013).
[14] A. Vaezi, Phys. Rev. B **87**, 035132 (2013).
[15] L. H. Santos and T. L. Hughes, Phys. Rev. Lett. **118**, 136801 (2017).
[16] Y.-Z. You and X.-G. Wen, Phys. Rev. B **86**, 161107(R) (2012).
[17] M. Barkeshli, C.-M. Jian, and X.-L. Qi, Phys. Rev. B **87**, 045130 (2013).
[18] M. Barkeshli, C.-M. Jian, and X.-L. Qi, Phys. Rev. B **88**, 235103 (2013).
[19] J. Klinovaja and D. Loss, Phys. Rev. B **90**, 045118 (2014).
[20] J. Klinovaja and D. Loss, Phys. Rev. Lett. **112**, 246403 (2014).
[21] J. Klinovaja, A. Yacoby, and D. Loss, Phys. Rev. B **90**, 155447 (2014).
[22] M. Barkeshli and X.-L. Qi, Phys. Rev. X **4**, 041035 (2014).
[23] M. Barkeshli, Y. Oreg, and X.-L. Qi, arXiv:1401.3750.
[24] M. Barkeshli, P. Bonderson, M. Cheng, and Z. Wang, arXiv:1410.4540.
[25] M. Burrello, B. van Heck, and E. Cobanera, Phys. Rev. B **87**, 195422 (2013).
[26] J. Motruk, E. Berg, A. M. Turner, and F. Pollmann, Phys. Rev. B **88**, 085115 (2013).
[27] R. Bondesan and T. Quella, J. Stat. Mech. (2013) P10024.
[28] A. S. Jermyn, R. S. K. Mong, J. Alicea, and P. Fendley, Phys. Rev. B **90**, 165106 (2014).

[29] A. Milsted, E. Cobanera, M. Burrello, and G. Ortiz, Phys. Rev. B **90**, 195101 (2014).

[30] E. M. Stoudenmire, D. J. Clarke, R. S. K. Mong, and J. Alicea, Phys. Rev. B **91**, 235112 (2015).

[31] Y. Zhuang, H. J. Changlani, N. M. Tubman, and T. L. Hughes, Phys. Rev. B **92**, 035154 (2015).

[32] G. J. Sreejith, A. Lazarides, and R. Moessner, Phys. Rev. B **94**, 045127 (2016).

[33] E. Cobanera, J. Ulrich, and F. Hassler, Phys. Rev. B **94**, 125434 (2016).

[34] Paul Fendley, J. Phys. A **47**, 075001 (2014).

[35] P. Fendley, J. Stat. Mech. (2012) P11020.

[36] A. Alexandradinata, N. Regnault, C. Fang, M. J. Gilbert, and B. A. Bernevig, Phys. Rev. B **94**, 125103 (2016).

[37] A. Hutter and D. Loss, Phys. Rev. B **93**, 125105 (2016).

[38] E. Cobanera and G. Ortiz, Phys. Rev. A **89**, 012328 (2014).

[39] E. Cobanera, arXiv:1410.5824.

[40] D. Perez-Garcia, F. Verstraete, M. M. Wolf, and J. I. Cirac, Quantum Inf. Comput. **7**, 401 (2007).

[41] H. Katsura, D. Schuricht, and M. Takahashi, Phys. Rev. B **92**, 115137 (2015).

[42] S. Ostlund, Phys. Rev. B **24**, 398 (1981).

[43] D. A. Huse, Phys. Rev. B **24**, 5180 (1981).

[44] V. A. Fateev and A. B. Zamolodchikov, Phys. Lett. A **92**, 37 (1982).

[45] F. C. Alcaraz, J. Phys. A **20**, L623 (1987).

[46] G. Ortiz, E. Cobanera, and Z. Nussinov, Nucl. Phys. **B854**, 780 (2012).

[47] R. S. K. Mong, D. J. Clarke, J. Alicea, N. H. Lindner, and P. Fendley, J. Phys. A **47**, 452001 (2014).

[48] D. S. Rokhsar and S. A. Kivelson, Phys. Rev. Lett. **61**, 2376 (1988).

[49] C.-H. Lin and M. Levin, Phys. Rev. B **92**, 035115 (2015).

[50] N. Lang and H. P. Büchler, Phys. Rev. B **92**, 041118 (2015).

[51] F. Iemini, L. Mazza, D. Rossini, R. Fazio, and S. Diehl, Phys. Rev. Lett. **115**, 156402 (2015).

[52] See Supplemental Material at http://link.aps.org/supplemental/10.1103/PhysRevLett.118.170402 for details on the definition of Fock parafermions, on the diagonalization of the model at $\phi = 0$, and on the analytical computation of observables including the perturbative form of the weak edge modes.

[53] Z. Nussinov and G. Ortiz, Ann. Phys. (Amsterdam) **324**, 977 (2009).

[54] U. Schollwöck, Rev. Mod. Phys. **77**, 259 (2005).

[55] J. Kurmann, H. Thomas, and G. Müller, Physica (Amsterdam) **112A**, 235 (1982).

[56] G. Müller and R. E. Shrock, Phys. Rev. B **32**, 5845 (1985).

[57] S. M. Giampaolo, G. Adesso, and F. Illuminati, Phys. Rev. Lett. **104**, 207202 (2010).

[58] I. Peschel and T. T. Truong, J. Stat. Phys. **45**, 233 (1986).